Homogeneous Freestanding Luminescent Perovskite Organogel with Superior Water Stability

Yucheng Zhang, Yusen Zhao, Dong Wu, Jingjing Xue, Yu Qiu, Michael Liao, Qibing Pei, Mark S. Goorsky, and Ximin He*

Metal-halide perovskites have become appealing materials for optoelectronic devices. While the fast advancing stretchable/wearable devices require stability, flexibility and scalability, current perovskites suffer from ambient-environmental instability and incompatible mechanical properties. Recently perovskite–polymer composites have shown improved in-air stability with the protection of polymers. However, their stability remains unsatisfactory in water or high-humidity environment. These methods also suffer from limited processability with low yield (2D film or beads) and high fabrication cost (high temperature, air/moisture-free conditions), thereby limiting their device integration and broader applications. Herein, by combining facile photo-polymerization with room-temperature in-situ perovskite reprecipitation at low energy cost, a one-step scalable method is developed to produce freestanding highly-stable luminescent organogels, within which $CH_3NH_3PbBr_3$ nanoparticles are homogeneously distributed. The perovskite-organogels present a record-high stability at different pH and temperatures, maintaining their high quantum yields for > 110 days immersing in water. This paradigm is universally applicable to broad choices of polymers, hence casting these emerging luminescent materials to a wide range of mechanical properties tunable from rigid to elastic. With intrinsically ultra-stretchable photoluminescent organogels, flexible phosphorous layers were demonstrated with > 950% elongation. Rigid perovskite gels, on the other hand, permitted the deployment of 3D-printing technology to fabricate arbitrary 2D/3D luminescent architectures.

Organometal halide perovskites have attracted extensive attention in the past decade owing to their excellent performance as active layers in photovoltaic devices.[1] Also, their attractive intrinsic optical properties, such as bandgap tunability, long carrier lifetime, high photoluminescence quantum yield, and narrow emission linewidths,[2] render them promising materials for display applications. Using perovskite quantum dots (PQDs) or perovskite nanoparticles (PNPs) including all-inorganic (e.g., $CsPbX_3$) and organic–inorganic (e.g., $CH_3NH_3PbX_3$) ones, a broad range of high-performance solar cells,[3] light emitting diodes (LED),[4] lasing,[5,6] waveguides,[7] photodetectors,[8,9] and field effect transistors[10] have been developed in recent years.

Accompanied by the excellent performance of PNPs come the undesirable material stability issues. The low formation energy of the material and highly mobile ionic structure with surface traps[11] make perovskites vulnerable to external factors including light, moisture, and temperature. The poor stability has become the major obstacle for the practical application of PQD-based solar cells, LEDs and other devices, whose performance often drop drastically, down to a few hours in ambient environment.[12] Moreover, traditional device fabrication and testing utilize pre-formed PNPs, which require oxygen/moisture-free environment[13] and high temperature[14] for synthesis and postannealing treatment, associated with high energy consumption. Addressing these instability issues, while maintaining the versatile processibility of these perovskite nanomaterials, may offer tremendous opportunities to optoelectronics and energy science. It is highly desirable to achieve in situ and simultaneous formation and protection of PNPs in a one-pot synthesis (where PNPs are formed being protected), which is suitable for large-scale industrial manufacturing with a low energy cost.

Recently many strategies have been explored for stabilizing the perovskite materials exposed to various harsh environments. For instance, surface modification including shape-preserving transformation,[15] oligomeric ligand functionalization,[16] and silica matrix encapsulation[4] have been reported to improve the stability, but PNPs in those demonstrations are not fully water resistant. Dense waterproof polymers, such as polystyrene, were

Y. Zhang, Y. Zhao, D. Wu, J. Xue, Dr. Y. Qiu, M. Liao, Prof. Q. Pei, Prof. M. S. Goorsky, Prof. X. He
Department of Materials Science and Engineering
University of California
Los Angeles, CA 90095, USA
E-mail: ximinhe@ucla.edu
Prof. X. He
California Nanosystems Institute
Los Angeles, CA 90095, USA

used to encapsulate and protect PNPs against moisture. Also, fluorescent polymer composites with lanthanide ions, organic dyes, or quantum dots (QDs) as the fluorescence centers have been broadly used in biosensing and optoelectronic devices. Embedding PNPs into the polymer matrix is a mutually beneficial process: the polymer matrix provides a protective structure to PNPs, and the PNPs endows the polymers with excellent optical properties, especially photoluminescent functions. In a recent report, a swelling–deswelling strategy was used to introduce presynthesized PNPs into spin coated polymer thin films to form the perovskite–polymer luminescent composites,[17] which enabled stable photoluminescence (PL) in water for two months. However, the spin-coating process limits the composite as 2D planar films. Such processing inflexibility severely restricts the applications of such luminescent polymers. More importantly, this two-step swelling–deswelling method resulted in perovskite dispersion in only a few micrometer thin surfacial region of the polymer film, yielding an inhomogeneous material containing a thin PNP-rich layer that occupies <10% of the entire polymer film thickness. Such a small fraction of active PNP layer in the polymer film limited the device efficiency. To overcome these disadvantages, PNP-embedded nanoscale polymer beads[18] were fabricated using the same swelling–deswelling method; however, the long-term water resistance was compromised undesirably, with a >50% PL-intensity drop within only one week. So far there is still no effective method to endow perovskite materials with both high water resistance and flexibility (i.e., structure designability and mechanical property tunability) at the same time. The increasing demands on various flexible or wearable optoelectronic devices, such as stretchable LEDs[19] necessitate the development of new perovskite materials with high stability and flexibility more urgent.

Compared to the previously used conventional polymer,[12,13] crosslinked polymers or gels can provide a more favorable 3D compact matrix to protect the embedded PNPs, by directly forming freestanding and scalable structure.[20] However, the intrinsic hydrophilicity of the conventional hydrogel system is incompatible to perovskites due to their sensitivity to moisture. Synthesis of PNPs in a gel matrix in a facile, scalable, and environment-stable manner has still not been realized.

Here, a homogeneous luminescent polymer organogel containing organic–inorganic PNPs, termed PNP gels, with record-high water resistance is reported. Inspired by the facile room-temperature PNP reprecipitation technique[21,22] and benefiting from the porous structure of polymer gels, we successfully developed a fast one-pot photopolymerization method for synthesizing luminescent polyacrylate organogels, which possess high quantum efficiency and excellent mechanical properties tunable from a highly stretchable gel of 950% elongation to a highly rigid gel of a 110 MPa modulus. The polymer organogels can be immersed in water and aqueous acid solution with no apparent PL quenching for more than three months. Practically, the high stability and designability allow the perovskite materials to successfully construct flexible LED devices with high efficiency and long-term durability. Furthermore, the simple photopolymerization process also makes the perovskite polymer 3D-printable. This new 3D printing ability opens up enormous opportunities for fabricating luminescent materials of arbitrary, complex 3D architectures, and rapid

low-cost manufacturing of optoelectronic devices with previously unachievable structures.

The matrix of the PNP gels is a crosslinked hydrophobic polymer with a porous network microstructure that possesses the freestanding nature and good elastic properties of the gel.[23] Instead of using traditional hydrophilic networks as in hydrogels, we selected hydrophobic polyacrylate as the matrix to embed and protect PNPs against ambient stress like moisture or general aqueous media. **Figure 1**a schematically shows the one-pot preparation of perovskite gels based on an on-site reprecipitation process. Specifically, to form an exemplary $CH_3NH_3PbBr_3$ ($MAPbBr_3$) NP–embedded poly(butyl acrylate) (PBA) gel, CH_3NH_3Br (MABr), and $PbBr_2$ are dissolved into dimethylformamide (DMF) solvent at a 3:1 molar ratio with oleic acid (OA) and oleylamine (OAm) as the ligands to form the perovskite precursor (solution A). Then, the acrylate precursor (solution B) is prepared by mixing acrylate monomer with the crosslinker N,N'-methylenebisacrylamide (BIS) and the photo-initiator 2-hydroxy-2-methylpropiophenone (Darocur 1173). By mixing the solution A and solution B, the PNP gel precursor is formed and can be photo-polymerized under UV light exposure into a transparent gel of desirable shape in a mold or by photolithographic 3D printer. Subsequently, the gel is immersed in toluene for solvent substitution. As the toluene gradually diffuses into the gel through those micropores, the gel swells for about twice in volume and the perovskite crystals start to nucleate and grow inside the gel matrix, due to the low solubility of the perovskite in toluene. Gradually, the color of the gel changes from transparent clear to opaque yellow–orange (Figure 1b). The as-obtained gel is dried in air for 4 hours to remove the solvent. During the solvent evaporation, the swollen and sticky gel shrinks back to the original size with a robust and rigid mechanical strength, indicating the completion of formation of a strong luminescent PNP gel composite (Figure 1c). The fabrication method of this luminescent PNP gels has been found to be facile and robust without the need of harsh condition, such as vacuum or high temperatures required in traditional methods. The entire gel preparation process is conducted in ambient condition under room temperature, with no additional protection or treatment.

Structural characterizations provide proofs that the PNPs are well dispersed throughout the entire 3D network of the gel. Scanning electron microscopy (SEM) images of both the surface and the internal structure of a typical gel with and without PNPs respectively are shown in Figure 1d–g. Both gels display identical typical porous structure, indicating that the embedding of NPs does not affect the morphology of the gel. Figure 1d,e shows the PNP gels contain nanoparticles of ≈100 nm diameter. By contrast, in the pristine PBA gel no such NPs is observed (Figure 1f,g). To verify the spatial distribution of the PNPs throughout the network, the interior cross-section of freshly cut PNP gels is imaged. As revealed by the morphology of the exterior and the interior surfaces of PNP gels respectively in Figure 1d,e, the PNPs are both uniformly dispersed in the gel matrix, suggesting the good protection of PNPs from the polymer matrix.

To further prove the encapsulation of PNPs in the polymer matrix and test the water stability of PNPs, the X-ray diffraction (XRD) pattern of the $MAPbBr_3$ NPs-at-PBA gel after immersion

**ADVANCED
SCIENCE NEWS**
www.advancedsciencenews.com

**ADVANCED
MATERIALS**
www.advmat.de
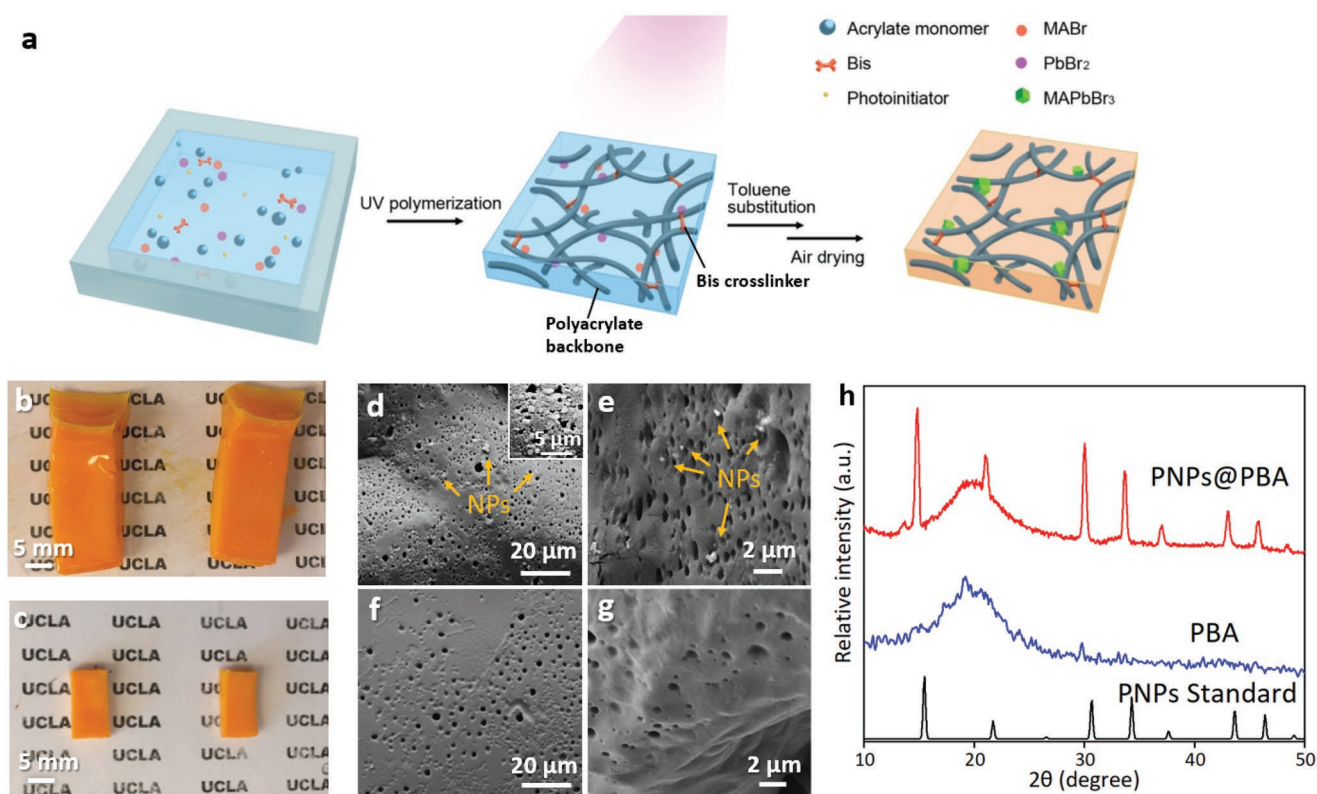
Figure 1. a) Schematic of the preparation of PNP gels, based on an on-site reprecipitation process. b,c) Photos of luminescent poly(butyl acrylate) (PBA) gel containing MAPbBr$_3$ NPs at, respectively, (b) 5 minutes and (c) 4 hours after taking out from toluene. d,e) The scanning electron microscopic (SEM) images of (d) interior surface and (e) exterior surface of the luminescent PNP gels. f,g) The SEM images of (f) interior surface and (g) exterior surface of the PBA gels without PNPs, as the control samples prepared under identical condition. h) The XRD patterns of MAPbBr$_3$ in the PBA gel, in comparison with the standard patterns of pure PBA and MAPbBr$_3$.[30]

in water for 40 days is compared with those of the pure PBA and MAPbBr$_3$, as shown in Figure 1h. The pattern of MAPbBr$_3$ NPs-at-PBA gel has a baseline similar to the blank PBA gel and peaks corresponding to the standard pattern of MAPbBr$_3$. This proves the encapsulation of PNPs in the polymer matrix with high water stability.

The photoluminescent performance of the PNP gels has been examined. A series of PNP gels made from precursor solutions of different MAPbBr$_3$ concentrations in DMF are measured, to study the influence of PNP-precursor concentration on the PL intensity (**Figure 2**a1, a2). As expected, the PL intensity of the PNP gel increases with the concentration of PNP precursor. The PL intensity change as a function of concentration is nonlinear, perhaps because the formation of PNPs in the gel is accompanied by the diffusion of toluene, taking away some PNPs (Figure 2d). Another noteworthy phenomenon is the redshift with a higher concentration PNP precursor solution; this could arise primarily from the self-absorption of emitted of photons known for high-perovskite-concentration materials.[24] When exceeding the concentration of 2.4%, the perovskite in OA/OAm precipitates and inhibits the curing of the gel as shown in Figure S3 in the Supporting Information.

Many previous works managed to improve the stability of PNPs in ambient air but failed to maintain the PL when in direct contact with liquid water.[25] Here encapsulating PNPs with the hydrophobic polyacrylate matrices successfully lead

to ultrahigh stability of the PNPs when exposed to ambient environment with high humidity and even when immersed in aqueous solutions. (see Figure S5 in the Supporting Information for hydrophobicity studies of the polyacrylate polymers). By contrast, PNPs embedded in relatively hydrophilic copolymer poly(acrylate-co-acrylamide) immersed in RT water lost its PL drastically in a control test (Figure S2, Supporting Information), which also indirectly proved the effect of hydrophobicity on protecting PNPs from water. To systematically examine its chemical- and thermal-stability when immersed in water, the PL intensity change of PNP gels as a function of time was monitored by measuring the PL spectra of the gels immersed in various aqueous systems during the period of 16 days, including deionized (DI) water (pH = 7) at room temperature (RT) and elevated temperature (60 °C), hydrochloric acid solutions (pH = 2 and pH = 4), and sodium hydroxide (NaOH) solutions (pH = 9 and pH = 12). As shown in Figure 2e,f, the PNP gels exhibited excellent intensity retention of 95.3% in water and 102% in acid solution of pH = 12 under room temperature for 16 days. This implies the negligible water permeability into the main body of the hydrophobic gels, when the polymer matrix thickness is greater than the size of embedded perovskite nanoparticles to ensure effective protection of the particle from exposed to water and stability (Figure S7, Supporting Information). Surprisingly, the PL intensity even increased for RT water in the first few days and for an acidic solution, probably

**ADVANCED
SCIENCE NEWS**

www.advancedsciencenews.com

**ADVANCED
MATERIALS**

www.advmat.de
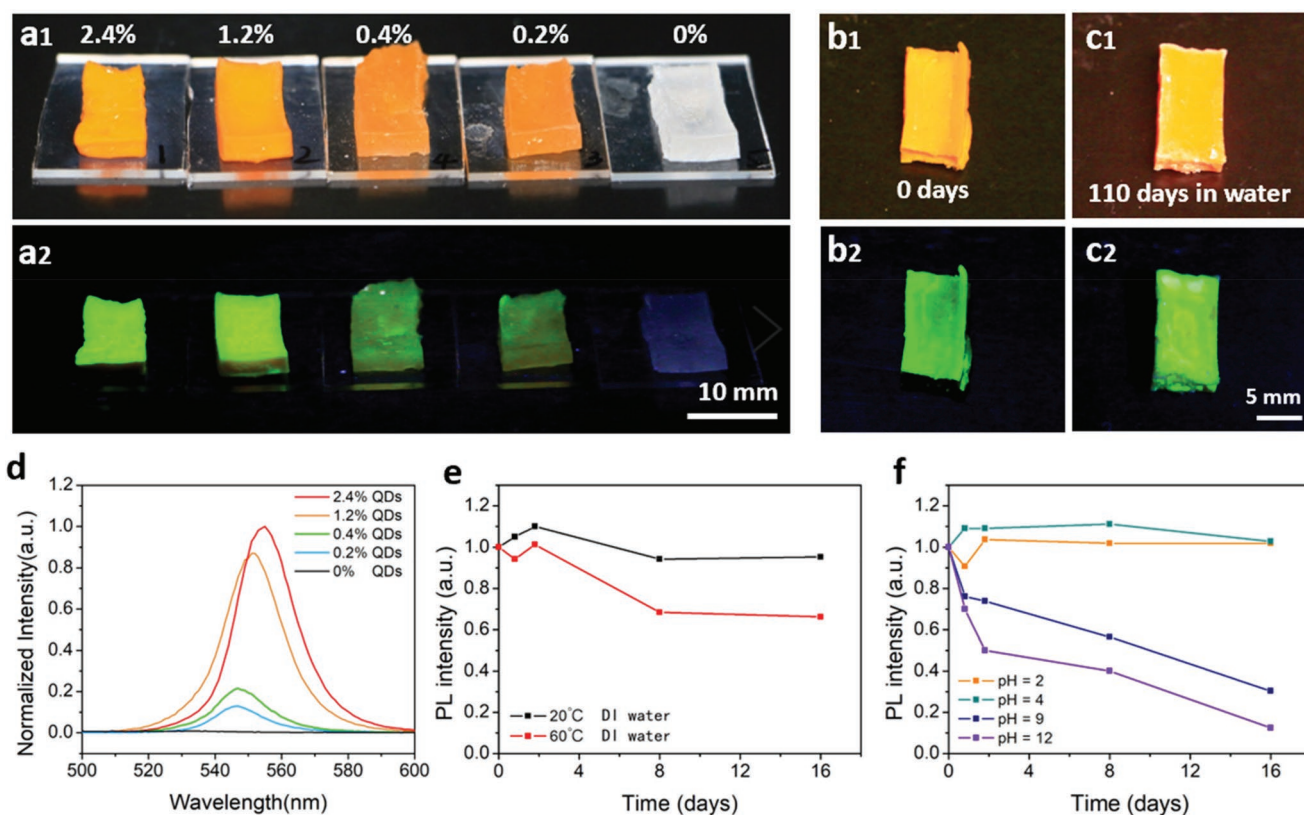
Figure 2. a1) The photographs of the corresponding luminescent PNP gels (MAPbBr$_3$ NPs-at-PBA gels) under indoor light and (a2) under 365 nm UV excitation in dark. The concentration of the PNPs in polymers in (a1) and (a2) tapers off from left to right. b1,c1) The comparison of photographs of the PBA gel with 2.4% PNPs before and after immersing in water at room temperature for 110 days under indoor light and (b2,c2) under 365 nm UV excitation in dark respectively. d) Normalized PL intensity of PNP gels in the matrix as a function of quantum dots molar ratio. e) The water resistance test of luminescent PNP gels immersed in 20 °C water and 60 °C water. f) The pH resistance of luminescent PNP gels at pH = 2, pH = 4 aqueous acid and pH = 9, pH = 12 aqueous alkali. The tested sample is PBA gels with 2.4% molar ratio of MAPbBr$_3$.

attributed to the photo enhancement, a typical phenomenon reported both in traditional nanoparticles and perovskite nanoparticles.[26] In the long-term stability test, we further found that the PL properties of the PNPs gels were well maintained after immersing in RT water for more than 110 days, as shown in Figure 2b1,b2,c1,c2. A distinct PL quenching for samples in 60 °C water and aqueous alkali was observed after 16 days, with the one in pH = 12 aqueous alkali showing the most PL intensity reduction. Such a loss of PL intensity was found to arise from the long-term thermal- and alkali-instability of PBA, as verified by the clear morphology change of the samples immersed in RT water, 60 °C water, and aqueous alkali for 20 days as shown in Figure S1 in the Supporting Information. The fracture surfaces of the latter two samples have been severely corroded by high-temperature or high-alkali aqueous environment, in contrast to the intact surface of the sample immersed in RT DI water. Thus, the corroded polymer matrix no longer provides hydrophobic protection for PNPs encapsulated in the matrix, which leads to the PL quenching. As a further test of thermal stability, the PNPs gels placed in high temperature environment showed the PL intensity was well maintained at 100 °C as shown in Figure S4 in the Supporting Information, while it dropped significantly at 150 °C in 1 hour, due to the intrinsic thermal instability of perovskite as previously reported.[27]

The traditional lead-containing perovskite, due to the hydrolysis of lead in aqueous environment, suffers from severe toxicity issues and limited applications in biomaterials and biomedical fields. Hence, beyond the presented promising long-term stability of the PNP gels, we examined the lead content changes in water before and after immersing the gels, using plasma-atomic emission spectrometry. The aqueous phases after gel immersion for 1 day and 20 days, respectively, have Pb^{2+} concentrations of 0.677 and 0.749 ppm, comparable to 0.663 ppm of blank DI water and well below the safe value of Pb^{2+} (1.931 ppm) for bioimaging applications.[13] This lead leaking test based on the Pb^{2+} concentration in the immersion liquids provides another proof for the firm encapsulation of PNPs in the polymer matrix and the superior water resistivity.

To demonstrate the universal applicability of our method for preparing luminescent PNP gels, a variety of luminescent PNP gels have been successfully synthesized using a series of acrylates as monomers (**Figure 3**a), including butyl acrylate (BA), poly(ethylene glycol) methyl ether acrylate (Acryl-PEG), ethyl acrylate (EA), methyl acrylate (MA), and 1,6-hexanediol diacrylate (HDODA). As shown in Figure 3b1,b2, the PNP gels are all in orange–yellow color under room light (Figure 3b1) and appear bright green under UV excitation throughout the entire body of the material (Figure 3b2), indicating high homogeneity

**ADVANCED
SCIENCE NEWS**

www.advancedsciencenews.com

**ADVANCED
MATERIALS**

www.advmat.de
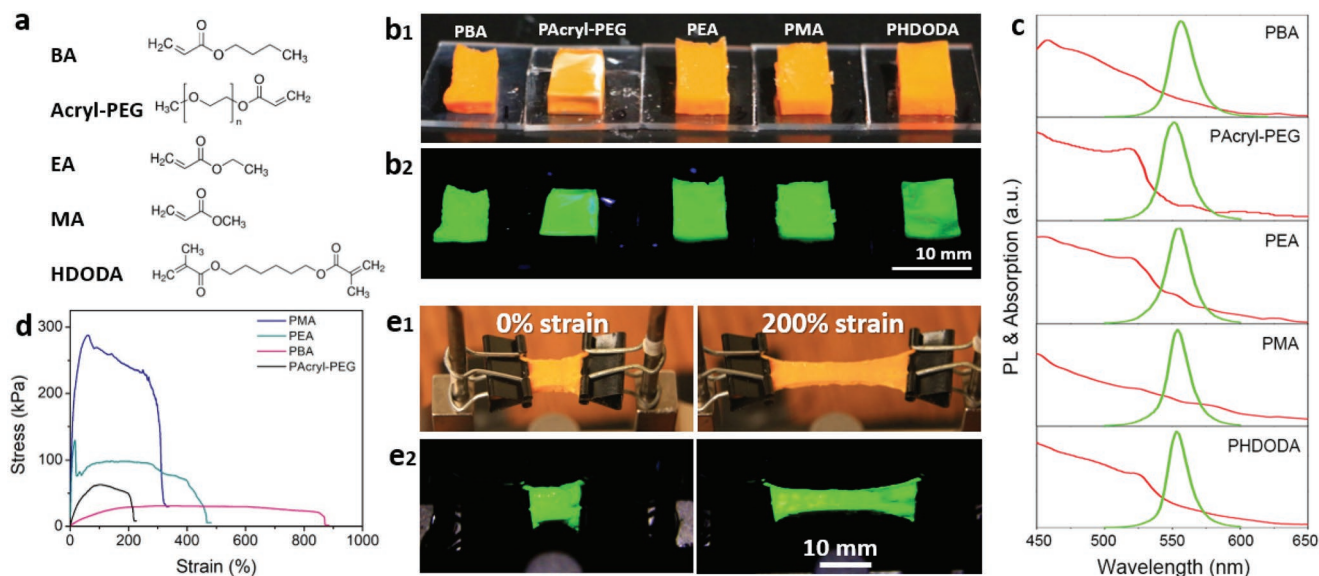
Figure 3. a) The chemical structures of a variety of acrylates used as monomers of PNP gels. They include butyl acrylate (BA), poly(ethylene glycol) methyl ether acrylate (Acryl-PEG), ethyl acrylate (EA), methyl acrylate (MA), 1,6-hexanediol diacrylate (HDODA). b1) The photographs of such luminescent polymer gels under indoor light. b2) the photographs of gels under 365 nm UV excitation in dark. c) The UV–vis absorption (red) and PL emission (green) spectra of PNP gels. d) Stress–strain curves of above PNP gels except HDODA. e1,e2) The stretchable PBA-based PNP gels under indoor light and UV irradiation.

of these composite materials. The PL emission wavelength in the range of 551–555 nm matches very well with the absorption onset wavelength located in the same range (Figure 3c). The full widths at half maximum (FWHM) of those gels are as narrow as 17–22 nm, which indicates the high purity of the generated green color. This narrow FWHM level outperforms the perovskite–polymer composite films prepared through the MAPbBr$_3$–polymer precursor mixture approach[28] (>30 nm) and through the swelling–deswelling approach (18–24 nm).[12]

Besides having excellent photoluminescent energy conversion efficiency, luminescent materials that can undergo large deformation, i.e., good tensile property, are highly desired especially for stretchable LEDs and many other flexible devices. A fatigue test on how strain affects the photoluminescent property as shown in Figure S6 in the Supporting Information proved the PL stability under cyclic tensile stress. On the other hand, a decent Young's modulus, instead, would be required for realizing 3D printing of complex luminescent structures. We have successfully realized this wide range of mechanical properties by designing a series of PNP gels with different polymer chain lengths, as their stress–strain curves shown in Figure 3d. As expected, the breaking elongation increases with the alkyl chain length. In the case of poly(butyl acrylate), the elongation at break exceeds 850%, while for poly(ethyl acrylate) and poly(methyl acrylate), the values are 468% and 322% respectively. This alkyl pendant-chain-length dependency of the breaking elongation is because longer pendant groups tend to limit the close chains to pack and increase the rotational mobility of the polymer chain,[29] resulting in the enhanced flexibility and stretchability of the overall gel network. Oppositely, lower alkyl pendant chain leads to higher Young's modulus but lower the tensile property. Using the PBA gel as a demonstration, we further examined the luminescent performance

of PNP gels under reversible stretching (200% strain) and recovery (Video S1, Supporting Information). Figure 3e shows photographs of a PBA-based PNP gel without stretching and at 200% strain. The stretched PNP gel presented uniform and bright illumination throughout the entire exposed area. With the demonstrated capability of making PNP gels with a broad spectrum of mechanical properties, from high stretchability to high strength, and luminescent properties under reversible stretching, this method serves as a broad-based platform for rational design of stretchable luminescent devices.

Based on the high stability, color purity, and material versatility, these luminescent materials with green color can be readily assembled as the down converter in the white-light LED (WLED) devices, where a blue LED pumps the red and green phosphor layers to generate white light (**Figure 4**a). As a simple demonstration, a PNP gel film and a red CdSe-at-PMMA film were deposited on a blue LED emitting at wavelength 454 nm with FWHM 20 nm, generating corresponding green light at wavelength 545 nm with FWHM 24 nm and red light at wavelength 637 nm with FWHM 29 nm and the resulted white light from a mixture of three primary colors as shown in Figure 4b. The spectral locus coordinates are (0.15, 0.021) as the bright blue color, (0.27, 0.72) as the emerald green color, and (0.71, 0.28) as the super red color are shown in Figure 4c, presenting great potentials for white-light-emitting devices. Additionally, the great stretchability with full mechanical reversibility of the luminescent PNP gels allows them to be alternative options to stretchable light emitting diodes.

Previous works focusing on the enhancement of stability of PNPs either encapsulate PNPs at the surface of polymer thin film through spin coating fabrication,[15] or wrap premade NPs within polymer beads forming luminescent powders.[16] These complex fabrication procedures and the lack of
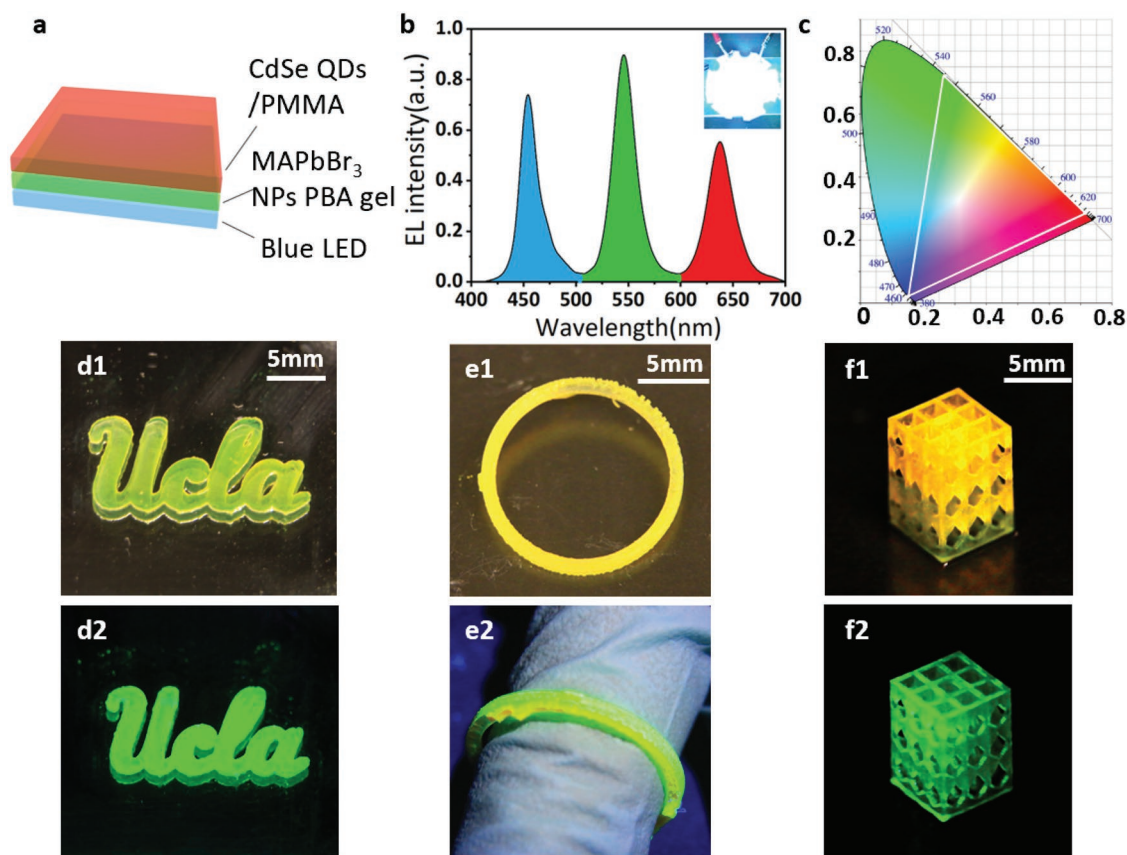
Figure 4. a) Graphic structure of the down-converter white-LED (WLED) device with a MAPbBr₃ NPs-at-PBA gel layer and red CdSe QD-at-PMMA as converter layers on a blue LED to generate white light. b) The emission spectra of a WLED device with a picture of the emitting device in the inset (scale bar = 1 cm). c) The color gamut of the WLED device in CIE1931. d–f) 2D patterns and 3D structures of MAPbBr₃ NPs-at-HDODA gels printed by a DLP-based 3D printer: (d1) 2D art characters "UCLA," (e1) ring and (f1) 3D lattice structure under white light, and (d2), (e2) and (f2) under UV light respectively.

substrates options in these methods severely limit the PNP composites to 2D structures or even lower dimensions. Compared to those restricted luminescent structures, the presented PNP gels can not only be prepared into the conventional 2D film devices as demonstrated in the WLED device, but also be fabricated into arbitrary complex 3D structures by 3D printing in a high-precision and time-effective fashion, giving credit to the simple photo-polymerization and the (solvent-induced) on-site reprecipitation process. Figure 4d–f showcases several examples of 2D patterns (Figure 4d1,d2) and 3D structures (Figure 4e1,e2,f1,f2) of printed luminescent gels using projection micro-stereolithography (PμSL). The favorable mechanical properties especially the rigidity, the low swelling ratio, and the ease of photopolymerization of PHDODA make it a qualified material for nearly all digital light processing (DLP)-based 3D printings. The combination of the new luminescent gel with 3D printing techniques opens the opportunities for preparing luminescent materials with arbitrary solid patterns and structures.

In summary, we have established a convenient and universal one-pot synthesis strategy to achieve ultrahigh water stability and tunable mechanical properties of perovskites, by in situ producing and embedding perovskite quantum dots into the hydrophobic polyacrylate matrix. This low-energy-cost strategy uses the facile room-temperature PNP reprecipitation technique with UV polymerization to obtain a photoluminescent gel with homogeneously distribute PNPs, maintaining the PL in water for more than three months. Fundamentally, this study has also advanced the understanding of perovskite stability and protection under various environmental conditions. The generality of our method and the modularity of the material design provide ample choices of polyacrylate or other gels with different mechanical properties, as well as various PNPs such as MAPbCl₃. To demonstrate the tunable mechanical properties (from elastic to rigid), highly stretchable phosphorous layers in a perovskite-based WLED device and several 3D-printed freestanding architectures were fabricated. Overall, this new method successfully enhanced the perovskite stability without compromising the processability and scalability as the expense. All these resulted in improvement of the overall (photo)electrical properties of perovskite materials; we believe this new kind of stable photoluminescent gels has huge potential in broad applications of optoelectronic devices. Broad choices of polymer matrix with super-hydrophobicity and thermal properties and other surface treatment methods could be further explored for realizing further optimized stability of perovskite materials.

Experimental Section

Fabrication of the Photoluminescent Gel with MAPbBr3 NPs in Polyacrylate, Using PBA as an Example: Precursor solution A was prepared by dissolving 3 mmol MABr and 1 mmol $PbBr_2$ into 15 mL DMF, with 0.9 mL OA and 60 µL OAm as ligands. The precursor A was then heated at 80 °C for 10 min under stirring. Precursor solution B was prepared by dissolving 10 mg BIS and 5 µL Darocur 1173 into 5.6 mmol BA (same mole amount monomer for MA, EA, and Acryl-PEG, 2.8 mmol for HDODA). 0.6 mL of precursor A was added to 0.8 mL of precursor B (0.520 mL for MA, 0.610 mL for EA, 0.630 mL for Acryl-PEG, and 0.420 mL for HDODA), and the mixture was injected to the designed model as a container for UV photo-polymerization. Both precursors were proved to be valid after 60 d storage under dark and 4 °C. A colorless gel was obtained by exposing the mixture of A and B under UV chamber for 180 s. The gel with PNPs was obtained by immersing the gel into toluene for at least 2 h and drying in the air for 4 h.

Fabrication of the Perovskite-Based WLED Device: A commercialized blue light LED (5W XLamp Cree XT-E Royal Blue 450–452 nm 20 mm XTE LED Light) was used as the blue light source. The green light layer on glass substrate was made by casting the precursor into a designed PDMS mold with an area of 20 mm × 20 mm and a thickness of 400 µm followed by UV curing. The red light layer was made by casting the mixed commercialized CdSe/ZnS quantum dots (Sigma-Aldrich, fluorescence λem 630 nm) with PMMA (950 PMMA A4) precursor into the same mold followed by thermal curing in a 50 °C vacuum oven for 4 h.

Characterizations: Scanning electron microscope characterizations were carried out with SUPRAU 40VP field emission scanning electron microscope (ZEISS Supra 40VP SEM). All samples were coated with Au before test without further treatments.

X-ray diffraction $2\theta{:}\omega$ scans were performed on a Bede high resolution X-ray diffractometer with a copper radiation source.

Steady-state photoluminescence (PL) spectra were obtained using Horiba Jobin Yvon system with some structural modification on sample loading part with excitation wavelength at 450 nm. All the measurements were carried out at room temperature.

The elongation-at-break test and Young's modulus measurement were conducted on the DMA (TA Instruments, Q800) at room temperature. The samples were the polyacrylate gels with PNP concentrations as mentioned above.

The emission spectra was characterized via a CCS 200 compact spectrometer.

3D Printing Process: A custom-built DLP-based 3D printer was used to print the 2D patterns and 3D structures of PNP gels in this work. The system consisted of a PRO4500 UV light (385 nm) projector (Wintech Digital System Technology Corporation), a motorized translation stage mounted to a motor controlled (Thorlabs, Inc.), and a computer program to control the system. The resolution of the 3D printer can achieve 30 µm on the *x–y* plane and 10 µm in the *z*-axis direction.

The 2D patterns as shown in the paper were one-step printed by projecting the light pattern for 15 s. For the ring structure and the 3D lattice structure, their CAD 3D models were first constructed and then sliced into serials of 2D images. The structures were printed layer by layer. Each layer was cured for 15 s. After printing, the samples were rinsed with toluene to precipitate the quantum dots trapped inside the polymers.

Supporting Information

Supporting Information is available from the Wiley Online Library or from the author.

Acknowledgements

Conflict of Interest

The authors declare no conflict of interest.

Keywords

[1] W. Yin, J. Yang, J. Kang, Y. Yan, S. Wei, *J. Mater. Chem. A.* **2015**, *3*, 8926.

[2] P. Gao, M. Grätzel, M. Nazeeruddin, *Energy Environ. Sci.* **2014**, *7*, 2448.

[3] J. Xue, J. W. Lee, Z. Dai, R. Wang, S. Nuryyeva, M. E. Liao, S. Y. Chang, L. Meng, D. Meng, P. Sun, O. Lin, *Joule* **2018**, *2*, 1866.

[4] C. Sun, Y. Zhang, C. Ruan, C. Yin, X. Wang, Y. Wang, W. Yu, *Adv. Mater.* **2016**, *28*, 10088.

[5] S. Chen, K. Roh, J. Lee, W. Chong, Y. Lu, N. Mathews, T. Sum, A. Nurmikko, *ACS Nano* **2016**, *10*, 3959.

[6] G. Xing, N. Mathews, S. Lim, N. Yantara, X. Liu, D. Sabba, M. Grätzel, S. Mhaisalkar, T. Sum, *Nat. Mater.* **2014**, *13*, 476.

[7] T. Cohen, T. Milstein, D. Kroupa, J. MacKenzie, C. Luscombe, D. Gamelin, *J. Mater. Chem. A* **2019**, *7*, 9279.

[8] L. Zhou, K. Yu, F. Yang, J. Zheng, Y. Zuo, C. Li, B. Cheng, Q. Wang, *Dalton Trans.* **2017**, *46*, 1766.

[9] L. Dou, Y. Yang, J. You, Z. Hong, W. Chang, G. Li, Y. Yang, *Nat. Commun.* **2014**, *5*, 5404.

[10] K. Wang, S. Dai, Y. Zhao, Y. Wang, C. Liu, J. Huang, *Small* **2019**, *15*, 1900010.

[11] A. Buin, P. Pietsch, J. Xu, O. Voznyy, A. Ip, R. Comin, E. Sargent, *Nano Lett.* **2014**, *14*, 6281.

[12] Y. Wei, Z. Cheng, J. Lin, *Chem. Soc. Rev.* **2019**, *48*, 310.

[13] M. Liu, M. Johnston, H. Snaith, *Nature* **2013**, *501*, 395.

[14] A. Mei, X. Li, L. Liu, Z. Ku, T. Liu, Y. Rong, M. Xu, M. Hu, J. Chen, Y. Yang, M. Gratzel, H. Han, *Science* **2014**, *345*, 295.

[15] T. Holtus, L. Helmbrecht, H. Hendrikse, I. Baglai, S. Meuret, G. Adhyaksa, E. Garnett, W. Noorduin, *Nat. Chem.* **2018**, *10*, 740.

[16] H. Huang, B. Chen, Z. Wang, T. Hung, A. Susha, H. Zhong, A. Rogach, *Chem. Sci.* **2016**, *7*, 5699.

[17] Y. Wang, J. He, H. Chen, J. Chen, R. Zhu, P. Ma, A. Towers, Y. Lin, A. Gesquiere, S. Wu, Y. Dong, *Adv. Mater.* **2016**, *28*, 10710.

[18] Y. Wei, X. Deng, Z. Xie, X. Cai, S. Liang, P. Ma, Z. Hou, Z. Cheng, J. Lin, *Adv. Funct. Mater.* **2017**, *27*, 1703535.

[19] S. Bade, X. Shan, P. Hoang, J. Li, T. Geske, L. Cai, Q. Pei, C. Wang, Z. Yu, *Adv. Mater.* **2017**, *29*, 1607053.

[20] K. Gattás-Asfura, Y. Zheng, M. Micic, M. Snedaker, X. Ji, G. Sui, J. Orbulescu, F. Andreopoulos, S. Pham, C. Wang, R. Leblanc, *J. Phys. Chem. B* **2003**, *107*, 10464.

[21] Y. Niu, F. Zhang, Z. Bai, Y. Dong, J. Yang, R. Liu, B. Zou, J. Li, H. Zhong, *Adv. Opt. Mater.* **2015**, *3*, 112.

[22] F. Zhang, H. Zhong, C. Chen, X. Wu, X. Hu, H. Huang, J. Han, B. Zou, Y. Dong, *ACS Nano* **2015**, *9*, 4533.

[23] L. Rogovina, V. Vasil'ev, E. Braudo, *Polym. Sci., Ser. C* **2008**, *50*, 85.

[24] Y. Fang, H. Wei, Q. Dong, J. Huang, *Nat. Commun.* **2017**, *8*, 14417.

[25] H. Zhang, X. Wang, Q. Liao, Z. Xu, H. Li, L. Zheng, H. Fu, *Adv. Funct. Mater.* **2017**, *27*, 1604382.

[26] D. deQuilettes, W. Zhang, V. Burlakov, D. Graham, T. Leijtens, A. Osherov, V. Bulović, H. Snaith, D. Ginger, S. Stranks, *Nat. Commun.* **2016**, *7*, 11683.

[27] A. Dualeh, P. Gao, S. Seok, M. Nazeeruddin, M. Grätzel, *Chem. Mater.* **2014**, *26*, 6160.

[28] D. Di, K. Musselman, G. Li, A. Sadhanala, Y. Ievskaya, Q. Song, Z. Tan, M. Lai, J. MacManus-Driscoll, N. Greenham, R. Friend, *J. Phys. Chem. Lett.* **2015**, *6*, 446.

[29] "Factors Tg", https://faculty.uscupstate.edu/llever/polymer%20resources/FactorsTg.htm (accessed: April 2019).

[30] A. Jaffe, Y. Lin, C. Beavers, J. Voss, W. Mao, H. Karunadasa, *ACS Cent. Sci.* **2016**, *2*, 201.